JOURNAL OF MATERIALS SCIENCE 20 (1985) 2973–2978

Dielectric and crystallization properties of massive amorphous selenium

M. F. KOTKATA, H. A. KHALEK*, W. M. ATIA*, T. PORJESZ‡, M. EL-SAMAHY
Physics Department, Ain Shams University, Cairo, Egypt
**Physics Department, Suez Canal University, Egypt*

The dielectric constant ε of amorphous selenium at 330 kHz has been measured under vacuum as a function of time on different isotherms T_a. After a normal heating period, depending on T_a, the value of ε increases abruptly from 5.8 to a maximum (9.6 to 11) followed by a decrease to reach a constant value. The behaviour of the curves $\varepsilon = f(t)$ is discussed in terms of the structural transformation in the amorphous matrix. The morphological changes during the spherulite growth of selenium are also discussed. The dielectric loss $\tan\delta$ has been calculated during the crystallization stages using the mesurements of time-dependence of resistivity $r(t)$. The crystallization kinetic parameters have also been computed from the variation of ε during the growth stage. A value of 1.2 eV is obtained for the activation energy of the radial growth of selenium in the temperature range 90 to 140° C.

1. Introduction

Crystallization in amorphous materials has been studied using various techniques. These include electron diffraction and microscopy [1], differential thermal analysis [2, 3], photoemission and optical absorption [4, 5], electrical [6–8] and thermal [9] conductivities, density and hardness [10], and magnetic susceptibility measurements [11]. The overall crystallization process can be studied by noting the weight fraction during both the isothermal and non-isothermal crystallization techniques. Experimental results which are obtained using either technique are conventionally interpreted in terms of the Avrami equation [12–14].

Amorphous selenium (*a*-Se) has a strong tendency to crystallize. The system *a*-Se transforms to the crystalline by evolving heat of transformation, if it is heated above $\approx 80°$ C but below its melting point of 220° C. Selenium crystallization normally proceeds via the formation of spherulites having a lamellar structure, with the width of the lamellae much less than the length of the extended selenium chain. This accommodation of selenium chains is affected by the repeated folding of the chains, giving rise to spherulites having a series of concentric rings. A spherulite is a spherically symmetrical formation made of radial rays diverging from the centre. Spherulites grow in crystallization under conditions of high viscosity or great supersaturation of the medium.

The aim of the present work was to use the dielectric constant, as a structural sensitive parameter, to follow the amorphous–crystalline transformation in massive *a*-Se and to obtain the Avrami kinetic parameters of the crystallization process.

2. Experimental details

The measuring technique consists in determining, with the help of a specially designed highly sensitive resonance circuit, the overpotential factor Q and the capacitance C. The method depends on a comparison between the capacitance C_0 of the cell measured empty, and the

‡*Permanent address*: Department for Low Temperature Physics, Roland Eötvös University, Budapest, Hungary.

0022–2461/85 $03.00 + .12

value C measured with the semiconducting material (selenium) inserted between its electrodes. The ratio C/C_0 gives the relative dielectric constant ε.

A graphite measuring cell made of spectroscopically pure rods was designed. It consists of two cylindrical graphite electrodes made coaxial at 1 mm spacing with the aid of a ceramic cover acting as a guard ring. A suitable amount of pure element selenium (99.999% purity) was inserted between the cell electrodes and fused at 300° C for 1 h in an evacuated (10^{-4} mm Hg) pyrex glass enclosure. The latter is provided with a chromel–alumel thermocouple and two tungsten leads, each of which is attached to one of the electrodes. A temperature control system was used to adjust the temperature of the cell with an accuracy better than 0.5° C. The molten selenium was quenched in iced water to obtain cylindrical samples in the amorphous state. The value of ε for the initial amorphous (as-prepared) selenium was determined by using a Schering bridge.

The change of the dielectric constant during the amorphous–crystalline transformation was recorded continuously as a function of time t for different annealing isotherms in the temperature range 90 to 160° C. A constant frequency of 330 kHz was used during all measurements. The function $\varepsilon = f(t)$ was found to be reproducible to better than 2%.

3. Results and discussion

Fig. 1 shows the time variation of the real part of the dielectric constant ε for a-Se isothermally annealed at 140° C (as an example). Similar behaviour to that of Fig. 1 was obtained for the other annealing temperatures investigated in the range 90 to 160° C.

In Fig. 1, variation of the function $\varepsilon = f(t)$ passes through three different time-dependent stages. The value of ε indicates first a small decrease (Region AB) as a result of the normal heating of the cylindrical selenium condenser from room temperature to the preheated temperature of the oven (annealing temperature, T_a). After a certain period, depending on T_a, the value of ε rises rapidly from 5.7 to attain a certain maximum (10.55 at 140° C). Such an increase inε (Region BC) is due mainly to transformation of the very high resistivity a-Se phase ($3.2 \times 10^8\,\Omega$cm) into a rather better conducting

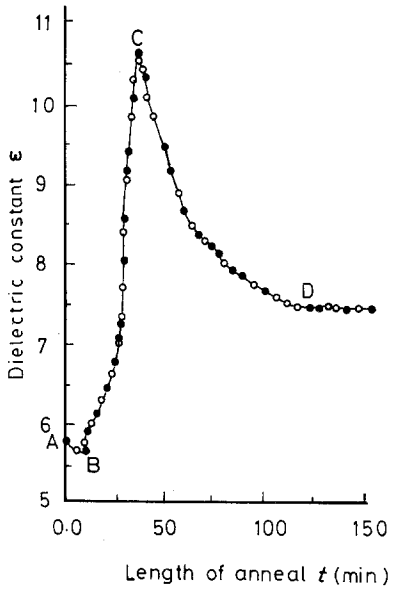

Figure 1 Annealing time dependence of ε for a-Se during its phase transformation at 140° C. ○ Run 1, ● Run 2.

(crystallized) state ($\varrho = 3 \times 10^2\,\Omega$cm at 140° C). This process is accompanied by a smooth liberation of heat energy associated with the transformation from a non-equilibrium thermodynamic state to a more equilibrium one. That is, this growth stage (BC) is nearly finished at the maximum point of the curve $\varepsilon = f(t)$. After Point C the dielectric constant shows a decrease until it reaches a constant limiting value at Point D (7.6 at T_a = 140° C). Such a decrease in ε (Region CD) is accompanied by a reduction in the ratio of surface to volume of the crystal grains. Champness and Hoffmann [15] related a similar decrease in the function $\sigma = 1/\varrho = f(t)$, after attaining a maximum value, to the process of incompleteness of crystallization of selenium. In this respect, we believe that the decrease of ε with the increasing of annealing time after reaching a maximum value at Point C is due to a progressive alignment of the spherulite branches of selenium. This stage is called *secondary crystallization* during which the spherulite structure becomes more perfect and the melt, which has hitherto remained uncrystallized between the structural elements of a spherulite, crystallizes further. The growth mechanism during crystallization of a-Se has been described by Crystal [16] and Kawarada and Nishina [17].

The change of T_a affects the time necessary for the different stages of transformation.

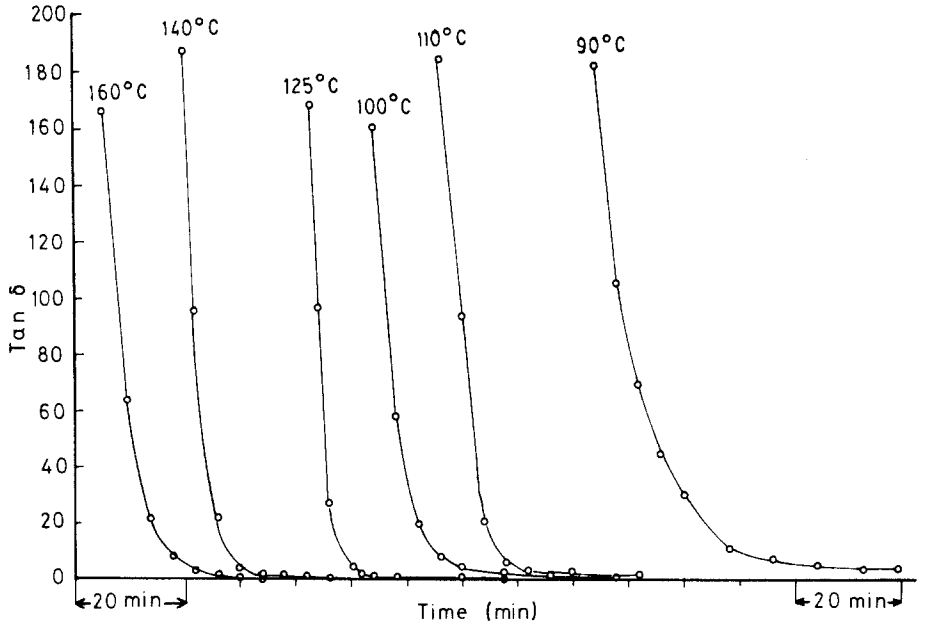

Figure 2 Annealing time dependence of $\tan\delta$ during the two stages of crystallization of *a*-Se crystallized on different isotherms. This corresponds to the path BCD in Fig. 1.

Increasing T_a from 90 to 160° C leads to a decrease in the normal heating period from about 40 min to zero. The period of radial growth (*primary crystallization* stage, Region BC) shows a decrease with T_a from 55 min at 90° C to 28 min at 140° C, then increases to 45 min at 160° C. Also, the temperature dependence of the total time of crystallization τ showed a minimum time to crystallize at 140° C. The value of τ decreases from 95 min at T_a = 90° C to 38 min at 140° C, then increases to 45 min at 160° C. Similar behaviour with a minimum time has been found for the crystallization of *a*-Se using other different isothermal techniques [18].

The initial value of ε is 5.8 $\pm$ 0.1. The maximum and final values of ε on the curves $\varepsilon = f(t)$ show respective changes of 9.6 to 11 and 7.2 to 7.8, depending on T_a. The latter affects the degree of crystallinity of the crystallized selenium samples [19].

During crystallization the specimen has a heterogeneous structure consisting of the original amorphous phase and hexagonal crystallites which are continually increasing in volume and have different electrical characteristics from those of the original phase. The dependence of the electrical conductivity σ of *a*-Se on time for different fixed temperatures of crystallization has been found experimentally [20]. Therefore, σ and ε are functions of the time of crystallization which itself depends on the strength of the electric field.

The energy loss parameter $\tan\delta$ can be found from the equation [21]

$$\tan\delta = \frac{1}{\omega C_p r_p} + \omega C_s r_s$$

where the dielectric is replaced by a loss-free dielectric and an active resistance connected in parallel (p) or in series (s). When ω is small, $1/\omega C_p r_p \gg \omega C_s r_s$ and so $\tan\delta = 1/\omega C_p r_p$; when ω is large (the present case), $1/\omega r_p C_p \ll \omega r_s C_s$ and so $\tan\delta = \omega r_s C_s$.

Calculations of the dependence of the dielectric loss inside the selenium with time of annealing during the two stages of crystallization were made from the above equation by using the appropriate values of $\varepsilon(t)$ and $r(t)$. The latter was obtained from the measurements of isothermal time-dependence of conductivity σ in massive *a*-Se [20]. Variation of the function $\tan\delta = f(t)$ is shown in Fig. 2 for different temperatures. The pronounced decrease in $\tan\delta$ corresponds to the increase of both $\sigma(t)$ and $\varepsilon(t)$ during the radial growth stage of *a*-Se. The nearly constant low values of $\tan\delta$ correspond to the decrease in $\varepsilon(t)$ during the secondary crystallization process of selenium (Region CD

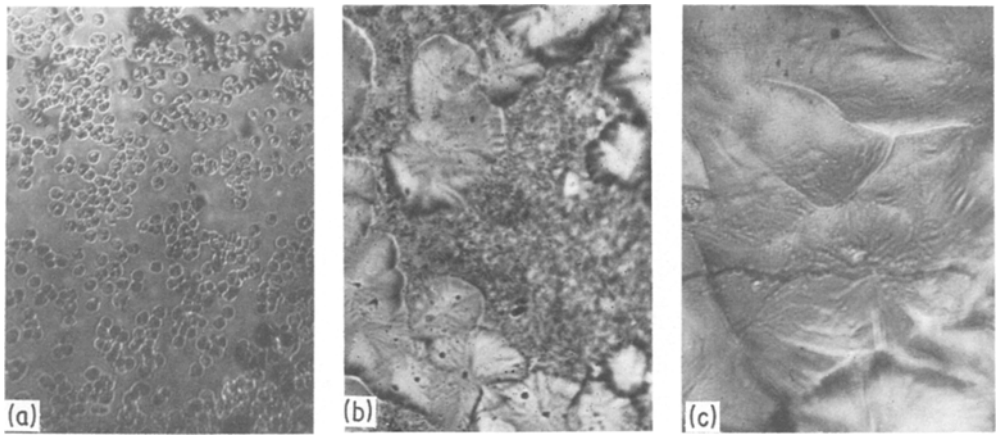

Figure 3 Optical photomicrographs illustrating growth of selenium films ($\approx 100\,\mu m$) during isothermal annealing, under vacuum, at 140° C for different times. (a) and (b) represent growth during the primary crystallization stage, and (c) corresponds to the secondary stage.

in Fig. 1). This drop in permittivity in the secondary process indicates that a major part of the driving force is a reduction in the field contribution to the bulk free energy.

Fig. 3 shows different stages of crystallization of *a*-Se films annealed at 140° C. The crystallization process starts at small centres distributed in the amorphous medium. These centres are gradually increased in size by increasing the crystallization time. It is clear also that the

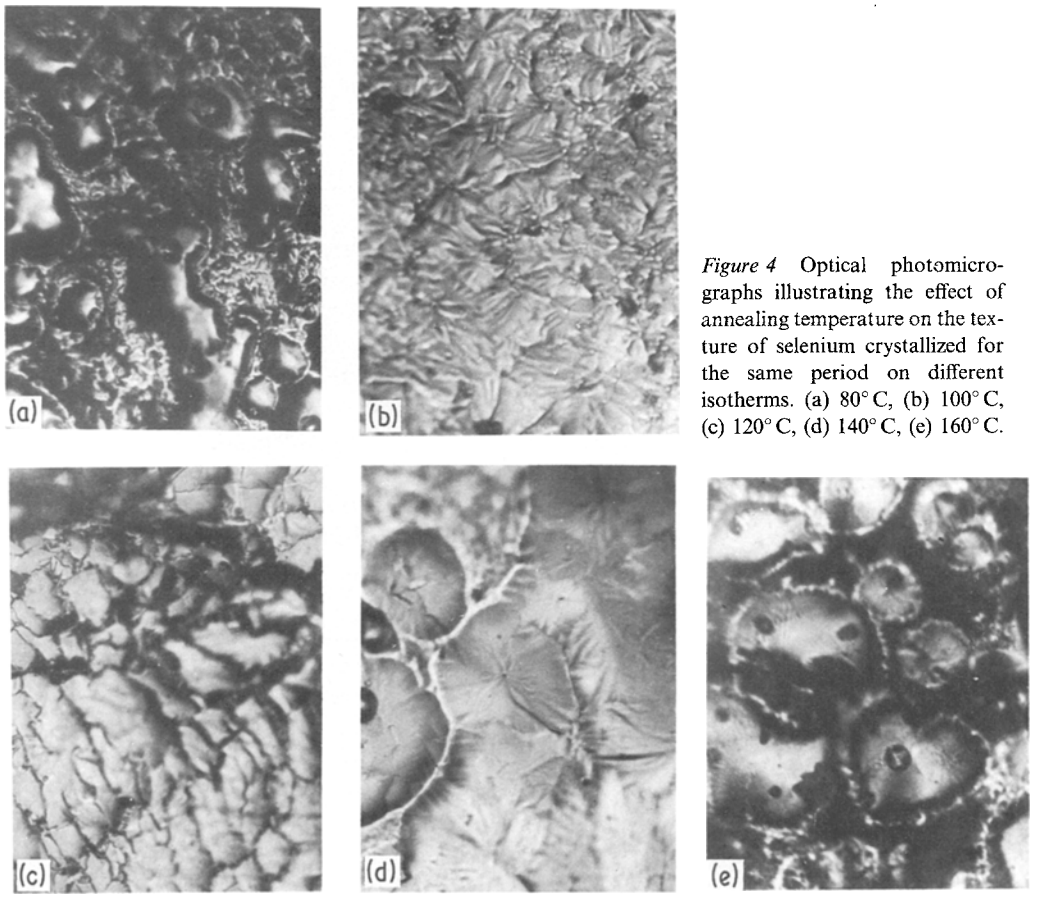

Figure 4 Optical photomicrographs illustrating the effect of annealing temperature on the texture of selenium crystallized for the same period on different isotherms. (a) 80° C, (b) 100° C, (c) 120° C, (d) 140° C, (e) 160° C.

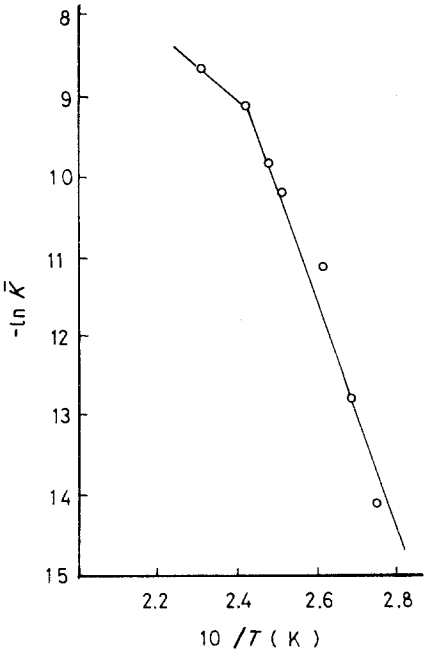

Figure 5 Dependence of ln $\bar{K}$ on reciprocal of absolute temperature T for selenium.

spherulites can swallow each other up during the growth process, as their number obviously decreases by increasing the annealing time. After a certain time, however, the growth process is almost complete and the crystallites appear with boundaries in contact with each other. A progressive aligning of the spherulite branches of selenium appears with further annealing. Of course, the temperature plays another role in controlling the rate of crystal growth. Fig. 4 shows the effect of T_a on the texture of selenium crystallized for the same period.

The dependence of the dielectric constant of selenium on time of crystallization has been used to calculate the transformed fraction α from the equation [22, 23]

$$\frac{1}{\varepsilon_t} = \frac{\alpha}{\varepsilon_a} + \frac{1-\alpha}{\varepsilon_c}$$

where $\alpha = V_a/V_0$; V_0 is the total volume of the specimen, V_a is the volume of the amorphous phase, and ε_a and ε_c are the values of ε for the amorphous and the crystallized phases. These phases correspond to Points B and C on the curve of Fig. 1. Here it is worth mentioning that at Point C more than 70% of the amorphous phase is crystallized.

The results of $\alpha = f(t)$ were used to calculate the kinetic parameters n and K of an Avrami equation of the form [12–14]

$$-\ln(1-\alpha) = Kt^n.$$

To fit the Avrami equation, a plot of $\ln[-\ln(1-\alpha_t)]$ against $\ln(t)$ must yield a straight line whose slope defines the crystallization mode n. The increase of T_a leads to a monotonic decrease in the value of n (from 2.22 to 1.36) up to 140° C. At $T_a = 160°$ C the value of n is found to be 1.5.

The activation energy E can be calculated from the temperature dependence of the rate of crystal growth $K(T)$ according to the equation

$$K(T) = K_0 \exp(-E/RT)$$

The relation between ln $\bar{K}$ (average over all values of K) for $\alpha \approx 0.15$ to 0.85 and $1/T$ is given in Fig. 5 where the plot shows two slopes. These correspond to 1.2 eV for the temperature range of 90 to 140° C, and 0.43 eV for the range 140 to 160° C. These values are in agreement with those obtained on the basis of other structurally sensitive parameters [24].

References

1. K. P. MAMEDOV and Z. NURIEVA, *Sov. Phys.–Crystall.* **12** (1968) 605.
2. J. GRENET, J. P. LARMAGNAC and P. MICHON, *Thin Solid Films* **67** (1980) 117.
3. M. F. KOTKATA and E. A. MAHMOUD, *Mater. Sci. Eng.* **54** (1980) 163.
4. C. G. RIBLING, D. T. PIERCE and W. E. SPEAR, *Phys. Rev.* **B4** (1972) 4417.
5. N. A. BLUM and C. FELDMAN, *J. Non-Cryst. Solids* **22** (1976) 29.
6. M. K. EL-MOUSLY, M. F. KOTKATA and S. A. SALAM, *J. Phys. C* **11** (1978) 1077.
7. M. F. KOTKATA, F. M. AYAD and M. K. EL-MOUSLY, *J. Non-Cryst. Solids* **33** (1979) 13.
8. P. GERMAIN, K. ZELLAMA, S. SQUELARD and J. C. BOURGOIN, *J. Appl. Phys.* **50** (1979) 6986.
9. M. K. EL-MOUSLY and M. F. KOTKATA, *Acta Phys. Hung.* **43** (1977) 117.
10. L. N. SUVOROVA, E. V. SHKOLNIKOV and Z. U. BORISOVA, *Inorg. Mater.* **12** (1976) 186.
11. J. TAUC, A. MENTH and D. L. WOOD, *Phys. Rev. Lett.* **25** (1970) 749.
12. M. AVRAMI, *J. Chem. Phys.* **7** (1939) 1103.
13. *Idem, ibid.* **8** (1940) 212.
14. *Idem, ibid.* **9** (1941) 177.
15. C. H. CHAMPNESS and R. H. HOFFMANN, *J. Non-Cryst. Solids* **4** (1970) 138.
16. R. G. CRYSTAL, *J. Polym. Sci.* **8** (1970) 2153.
17. M. KAWARADA and Y. NISHINA, *Jpn. J. Appl. Phys.* **14** (1975) 1519.
18. E. A. MARSEGLIA and E. A. DAVIS, *J. Non-Cryst. Solids* **50** (1982) 13.

19. M. F. KOTKATA and M. H. ALY, *Ind. J. Technol.* **22** (1984) 170.
20. M. F. KOTKATA, G. M. KAMAL and M. K. EL-MOUSLY, *ibid.* **20** (1982) 390.
21. A. GOSWAMI and A. P. GOSWAMI, *Thin Solid Films* **16** (1972) 175.
22. I. Kh. GELLER, B. T. KOLOMIETS and A. I. POPOV, *Neorg. Mater.* **11** (1975) 1936.
23. A. I. POPOV, *Phys. Chem. Glasses* **19** (1978) 43.
24. M. F. KOTKATA and M. K. EL-MOUSLY, *Acta Phys. Hung.* **54** (1983) 303.

Received 10 April
and accepted 15 October 1984